

Conflict-Cost Based Random Sampling Design for Parallel MRI with Low Rank Constraints

Wan Kim^a, Yihang Zhou^a, Jingyuan Lyu^a and Leslie Ying^a

^aDepartment of Electrical Engineering

The State University of New York at Buffalo, Buffalo, New York, USA

ABSTRACT

In compressed sensing MRI, it is very important to design sampling pattern for random sampling. For example, SAKE (simultaneous auto-calibrating and k-space estimation) is a parallel MRI reconstruction method using random undersampling. It formulates image reconstruction as a structured low-rank matrix completion problem. Variable density (VD) Poisson discs are typically adopted for 2D random sampling. The basic concept of Poisson disc generation is to guarantee samples are neither too close to nor too far away from each other. However, it is difficult to meet such a condition especially in the high density region. Therefore the sampling becomes inefficient. In this paper, we present an improved random sampling pattern for SAKE reconstruction. The pattern is generated based on a conflict cost with a probability model. The conflict cost measures how many dense samples already assigned are around a target location, while the probability model adopts the generalized Gaussian distribution which includes uniform and Gaussian-like distributions as special cases. Our method preferentially assigns a sample to a k-space location with the least conflict cost on the circle of the highest probability. To evaluate the effectiveness of the proposed random pattern, we compare the performance of SAKEs using both VD Poisson discs and the proposed pattern. Experimental results for brain data show that the proposed pattern yields lower normalized mean square error (NMSE) than VD Poisson discs.

Keywords: Compressed Sensing, Parallel Imaging, SAKE, random sampling, conflict cost

1. INTRODUCTION

Compressed sensing is introduced to enable exact recovery of sparse signals from data sampled below what the Shannon-Nyquist sampling theorem¹ requires. Compressed sensing becomes very useful in MRI² because it allows the image to be acquired with much faster speed. For success of compressed sensing, the sampling needs to satisfy the incoherent requirement. Random sampling of the k-space (data domain) has been adopted in Sparse MRI³ and many subsequent studies. It allows the aliasing artifacts to be noise-like such that they can be effectively removed using some nonlinear reconstruction algorithms. Many different random sampling patterns have been introduced such as power density function³, Poisson disk⁴⁻⁵, and variable density (VD) Poisson disk sampling⁶ in order to make the sampling more effectively and satisfy the incoherent requirement for compressed sensing.

The challenge in sampling pattern design is how to sample most efficiently. In MRI, we usually take advantage of the fact that most important information is around the low frequencies, especially zero frequency or direct current (DC), when we sample the Fourier domain (called k-space in MRI) of natural images. Therefore most random sampling methods consider full sampling in the center part and random sampling in the outer region.

Recently, Poisson disc sampling pattern or its advanced versions, VD Poisson sampling patterns have been used extensively. Poisson disc sampling pattern requires any two points to be separated by at least a minimum distance⁷. However, in the case of reduction factor of 2 or 3 which is typically used to obtain high quality reconstructions, it is difficult for all samples to satisfy the minimum distance requirement. This is because Poisson disc method usually uses dart throwing⁶ to generate the random pattern and the pattern can be arbitrary. Also it is usually computationally expensive to generate a Poisson disc pattern, which can be an issue for real implementation or experiments⁸.

In this work, we propose a new random sampling pattern using a probability model and cost function. In order to produce a desired random sampling pattern, we will first allocate samples to a set with the same probability using the probability function of a generalized Gaussian shape. We next will use a cost function to assign samples to points of the

least cost so as to make the sampling pattern more incoherent. Then we reconstruct a brain image using SAKE (simultaneous auto-calibrating and k-space estimation)⁹ with the proposed sampling pattern. We finally compare the performance of our random sampling mask with that of VD Poisson disk.

2. METHODS

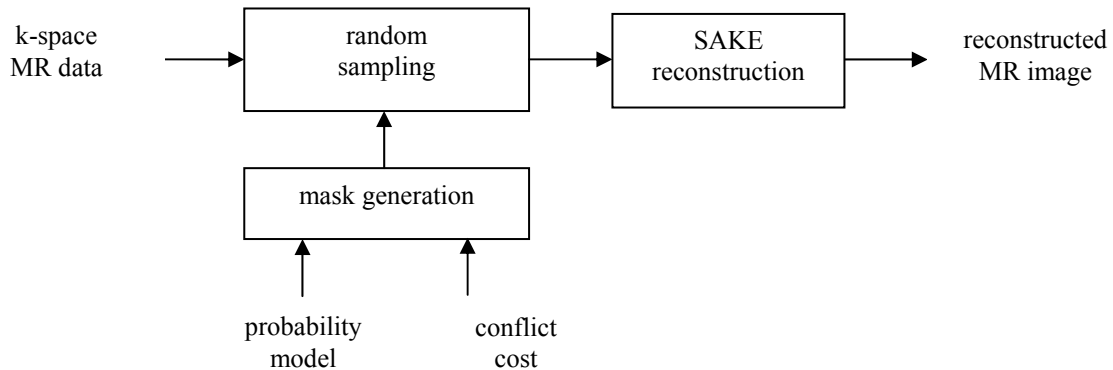


Figure 1. Flow chart of the reconstruction process

Figure 1 shows the whole process of the proposed reconstruction. We first generate a random sampling mask. Then we use the mask to randomly sample the k-space and apply SAKE to the sampled data to get the reconstruction image. The proposed method is explained in section 2.1 Probability Model, 2.2 Conflict Cost and section 2.2 Sample Selection Algorithm. The new method exploits a generalized Gaussian probability including a wide range of distributions from a uniform one to a Gaussian-like one centralized in a center frequency.

2.1 Probability Model

In order to control the distribution of sampling locations, one needs a probability model. Let $p(\vec{r})$ be the probability of assigning a sample to a spatial point \vec{r} where $\vec{r} = [r_x, r_y]$. Then $p(\vec{r})$ becomes the success probability of a Bernoulli random process. If $p(\vec{r})$ is a constant with regard to \vec{r} , then it shows a uniform distribution as in Poisson disks. As a good probability model, we choose an exponential function which is bounded in $[0, 1]$ while the power density function³, which is used in some conventional random sampling for compressed sensing, does not satisfy the bounded property. Introducing a shape parameter into the function as in a generalized Gaussian probability density function (pdf)¹⁰, we can control how much concentrated samples are around DC. Since DC and near-DC Fourier components contain meaningful information more than other regions, it is important to sample densely in those regions to produce good SNR.

The generalized Gaussian probability model of sample allocation using a shape parameter is formulated as

$$p(\vec{r}) = \exp \left\{ -\frac{1}{\mu_R} \left(\frac{\|\vec{r} - \vec{r}_0\|}{\|\vec{r}_0\|} \right)^\alpha \right\} \quad (1)$$

where \vec{r}_0 denotes a center point and α the parameter controlling the probability shape. The parameter μ_R depends on the reduction factor R , which satisfies the following constraint:

$$\sum_{\vec{r} \in I} p(\vec{r}) = \frac{|I|}{R}, \quad (2)$$

where I stands for the set of all locations in the whole k -space and $|I|$ the size of I . Also, Eq. (2) is equivalent to the total number of the samples. Given an R , the parameter μ_R is determined based on (2) not explicitly but by numerical iteration such as bisection method. The number of samples is an integer that is not exactly the same every time, but we can get a number close to the reduction factor. We will talk about this more on section 2.3.

Grouping all points into sets of points of the same probabilities, we rewrite (2) into the following:

$$\sum_n \sum_{\vec{r} \in S_n} p(\vec{r}) = \frac{|I|}{R}, \quad (3)$$

where $S_n, n=1,2, \dots$, represents the set of all points of the same probability. We now determine the number of samples to be allocated to the points of the same probability as

$$N_n = \sum_{\vec{r} \in S_n} p(\vec{r}). \quad (4)$$

2.2 Conflict Cost

Considering the incoherence requirement of compressed sensing, assigning samples purely randomly according to the probability model may not meet the incoherence requirements. To address the issue, we introduce conflict cost for each sample allocation in order to distribute samples evenly. We define the conflict cost of a point \vec{r} to a sample \vec{s} as

$$\Delta c(\vec{r}; \vec{s}) = e^{(-\gamma \|\vec{r} - \vec{s}\|)} \quad \text{for } \vec{r} \in B(\vec{s}), \quad (5)$$

where $B(\vec{s})$ denotes the set of neighbor points within a distance d around \vec{s} and γ the exponential slope parameter. The slope parameter should be larger than 0 because farther neighbor samples have to contribute less to the cost. Therefore, the total conflict cost of a point \vec{r} is obtained by summing the conflict costs between the point \vec{r} and all its neighbor samples.

2.3 Sample Allocation Algorithm

Let M be a sampling matrix, and initialize $M(\vec{r}) = 0$ for $\vec{r} \in I$. Whenever a sample is allocated to a point \vec{r} , the corresponding mask value becomes $M(\vec{r}) = 1$.

Next are the steps for the sample allocation algorithm based on the probability model and conflict cost.

Step 1: Initialize a sampling mask and a conflict cost array as $M(\vec{r}) = 0$ and $c(\vec{r}) = 0$ for $\vec{r} \in I$.

Step 2: Compute $p(\vec{r})$ for $\vec{r} \in I$ and the parameter μ_R according to (1) and (2).

Step 3: Group all points into sets S_n of points with the same probabilities, $n = 1, \dots, N_g$.

Step 4: Do the following operations for the set S_{N_g} of the highest probability to the set S_1 of the lowest probability.

(1) Compute the number of samples N_n to be allocated to S_n according to (4).

(2) Do the following operations for $m = 1$ to $m = N_n$.

- Sort the conflict costs of all points \vec{r} in S_n .

- Find the points of minimum conflict cost.

- If there are multiple minimum points, then select a point randomly and let it be \vec{s} .

- Set $M(\vec{s}) = 1$ and $c(\vec{s}) = \infty$.

- Set $c(\vec{r}) \leftarrow c(\vec{r}) + \Delta c(\vec{r}; \vec{s})$ for $\vec{r} \in B(\vec{s})$, where $\Delta c(\vec{r}; \vec{s})$ is given in (5).

The reason why we set the conflict cost of \vec{s} to be infinity is that the same point should not be selected as a sample point again in the following steps.

For more practical implementation, we need to round N_n in (4) into an integer because the number of samples should be an integer. However, excess or shortage in sum of probabilities caused by the integer rounding should be compensated in the next iteration. Especially, in case of $N_n = 0$ after rounding, we have to do $S_{n+1} \leftarrow S_n \cup S_{n+1}$. Next are the steps for the image reconstruction algorithm.

2.4 Image reconstruction

We use SAKE as an image reconstruction. SAKE is one of the parallel imaging reconstruction algorithms using low rank completion. Next is a brief review about SAKE.

Unlike GRAPPA¹¹, one of the well-known parallel imaging techniques, which needs ACS (auto calibration signal) lines to reconstruct images from undersampled multi-channel data, SAKE is an algorithm to reconstruct images from randomly undersampled data without calibration data. SAKE first connects all the coil data in series and the connected data are reformulated as the shape of the Hankel matrix used for Cadzow's signal enhancement. As a result, the reconstruction becomes a low rank matrix completion problem in k-space. The solution is obtained by singular value thresholding, especially hard-thresholding. The SAKE reconstruction is formulated as follows:

$$\begin{aligned} & \text{Minimize } \|Dx - y\|^2 & (6) \\ & \text{subject to } \text{rank}(A) = k, \\ & \quad x = H^+(A) \end{aligned}$$

where D denotes the sampling operation related to the sampling matrix M mentioned in section 2.3, x the desired image, y the acquired data, A the low-rank data matrix and H^+ the pseudo-inverse operator.

3. RESULTS

In order to evaluate the effectiveness of the proposed random masks, we compare the SAKE reconstructions using VD Poisson discs⁶ and the proposed random masks. The VD Poisson disk is generated from a Poisson disk using μ -law¹². Assuming samples are in the area of $[-1,1] \times [-1,1]$, each sample location is converted using

$$r' = \text{sgn}(r)(1 - |F(1 - |r|; \mu)|) \quad (7)$$

where r and r' denote the radius from the original sample location and the new location, respectively. The function $F(\cdot; \mu)$ means the μ -law of parameter μ . We generate Poisson disks using the Poisson disk generation code from the website <http://www.cs.virginia.edu/~gfx/pubs/antimony/>¹³. For fair comparison, we also used three masks provided by one of the authors of SAKE⁹, called Shin masks here. Figure 2 shows Shin and μ -law masks, where the parameter μ is chosen as $\mu=0.4(R-1)$. The μ -law patterns are shown to be very close to the Shin masks. We will use the VD Poisson disk with μ -law to compare with our proposed method for SAKE reconstruction. In the following experiments, we generate our masks and μ -law masks randomly fifty times at each reduction factor R to investigate the averaged behavior of the masks. Because of the way that the VD Poisson masks are generated, it is hard to get the exact reduction factor we want, while our masks show exact reduction factors. We place a fully sampled area called core in the center of all the masks and choose the circle of radius 3.

In (5), the slope parameter γ is set to be $\ln 4$ and the maximum neighbor distance $d=[1+R]$. The MRI data first used for test is the vivo axial brain data scanned on a 1.5T MRI scanner (GE, Waukesha, Wisconsin, USA) using an eight-channel receive-only head coil with data size 200×200 ⁹. The second scanned dataset was an axial brain image acquired on a GE 3T scanner (GE Healthcare, Waukesha, WI) using an 8-channel head coil with data size 256×256 from <http://www.acsu.buffalo.edu/~jlv27/>¹⁴.

Figure 3 shows the normalized mean square error (NMSE) of SAKE using the proposed mask with $R = 3.0$ according to the shape parameter α . The number of SAKE iterations is set to 15 for $\alpha > 0.5$, and to 100, 45, and 30 for $\alpha = 0, 0.2, 0.4$, respectively. In the figure, the NMSE of $\alpha = 1.0$ is shown to be minimum and other shape parameters yield higher NMSEs. We can see that NMSE of $\alpha = 1.0$ is somewhat less than that of $\alpha = 2.0$ which indicates Gaussian function. Figure 4 shows the masks according to various shape parameters α at $R=3$. The mask of $\alpha = 0$ is close to uniform random mask and $\alpha = 2.0$ shows the Gaussian mask. We see that one can easily control the concentration of samples around DC in the proposed mask by varying the shape parameter. The magnification of center parts of the masks is shown in figure 5. We can see that samples in the center part of our mask are more uniformly distributed and especially along circles than those of VD Poisson disks by μ -law and Shin.

The effect of conflict cost for the proposed generalized Gaussian (GG) mask is shown in Figure 6 as a function of the reduction factor R . Figure 6(a) shows the NMSE comparison of SAKE using the proposed mask with and without conflict cost. We can clearly see that our method with conflict cost has less noise than that without. Figure 6(b) shows the maximum correlation coefficients (MCC) between pixels and their eight nearest neighbors for reconstruction error images. Since the ideal reconstruction has noise-like reconstruction errors, we can say that the smaller MCC is, the more incoherent the sampling mask is¹⁵.

The normalized mean square errors (NMSEs) of various types of masks applied to SAKE according to $R=3.0$ are plotted in figure 7(a). The NMSEs curve for all method show the mean curve with the minimum and maximum for fifty masks. We see in the figure that the proposed random mask shows the best performance and least deviations all over the reduction factors. Figure 7(b) shows that the MCCs of our proposed masks are less than half of those of VD Poisson disk all over the reduction factors. The correlation coefficients for our proposed method are also shown to be less varied than those of VD Poisson disk. It suggests that our mask is more incoherent than the VD Poisson masks.

The experiments on the brain data⁹ are shown in figure 8. Our method using the proposed masks pattern reduces the reconstruction errors compared to the original method using the VD Poisson disks. Figure 9 shows the results from the second brain data. The NMSE using our sampling mask is below the mask used in the original SAKE paper. The reconstructed images of the brain using our method are more accurate than those using the VD Poisson disk.

4. CONCLUSION

We have proposed a new method to generate VD random sampling. Our masks have the following advantages over VD Poisson disks: Our method can always generate masks with a constant reduction factor, which means it is easy to control the number of samples with a parameter. Furthermore, our method is conceptually easy to implement using probability model and cost function satisfying the incoherence requirement. In addition, our proposed masks yield better image quality and lower NMSEs over VD Poisson disks. Future work will apply our proposed method to 3D MRI reconstruction or reconstruction of dynamic MR images in k-t domain.

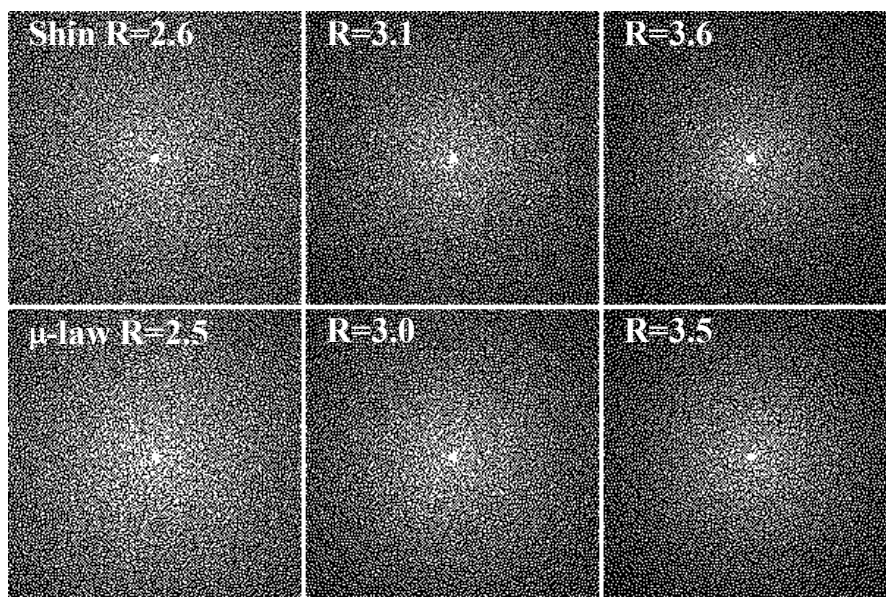


Figure 2. Shin and μ -law masks according to various reduction factor R .

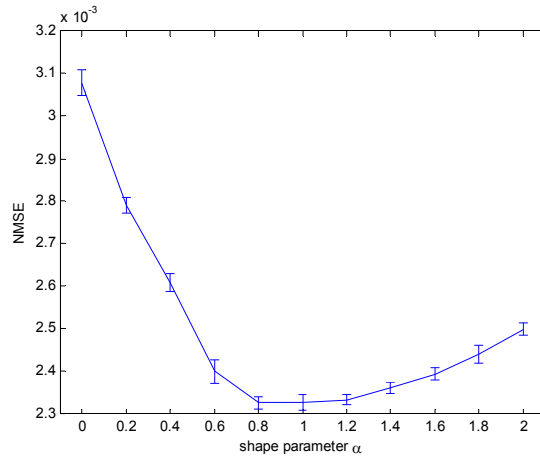


Figure 3. NMSE of SAKE reconstruction using the proposed random mask of $R=3.0$ as a function of the parameter α .

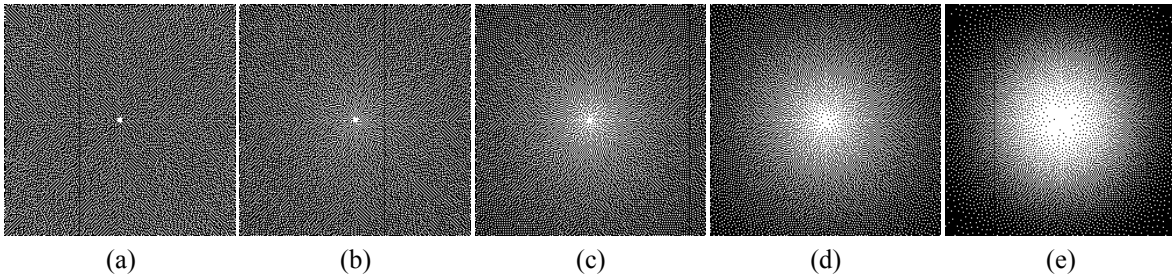


Figure 4. Proposed mask using different parameters α at $R=3$: (a) 0.0, (b) 0.2 (c) 0.5, (d) 1.0, and (e) 2.0.

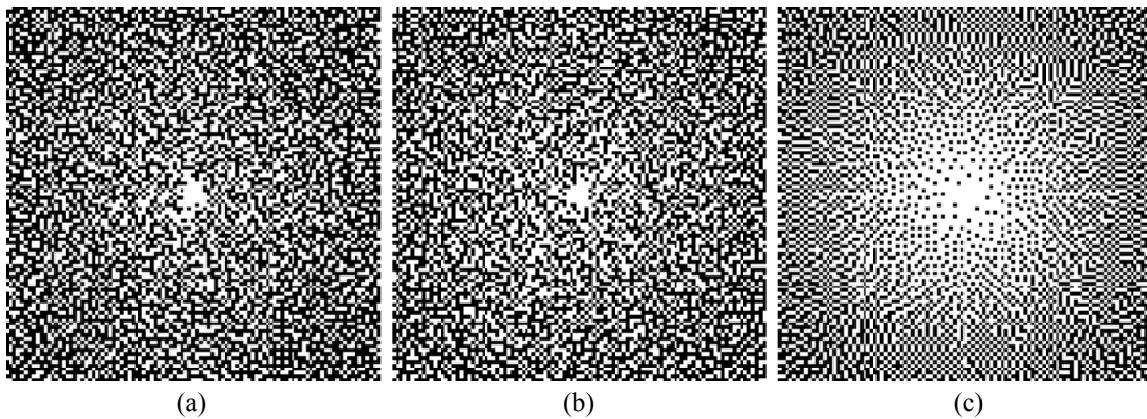
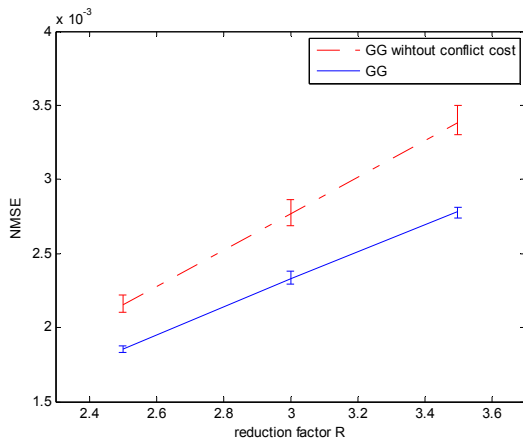
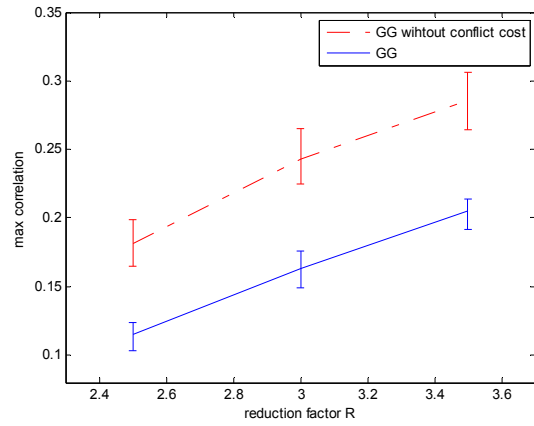


Figure 5. Zoomed-in center parts of different masks at $R=3$: (a) VD Poisson disk by Shin, (b) VD Poisson by μ -law, and (c) proposed mask.

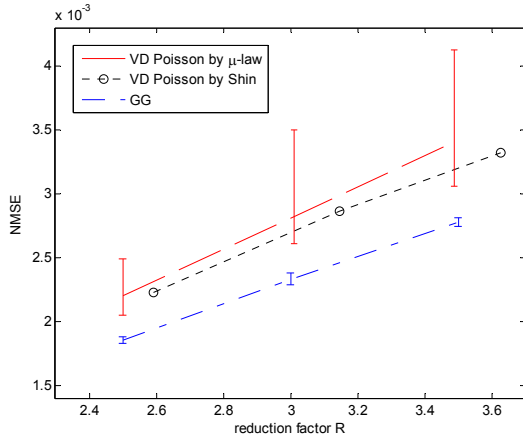


(a)

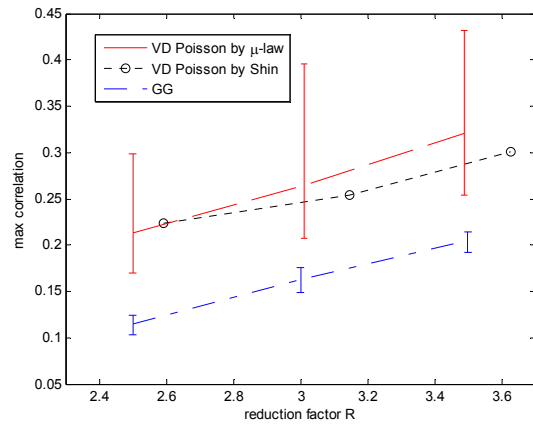


(b)

Figure 6. Effect of conflict cost. Comparison of SAKE reconstruction: (a) NMSEs and (b) maximum correlations using the proposed generalized Gaussian (GG) masks with and without conflict cost as a function of the reduction factor R .

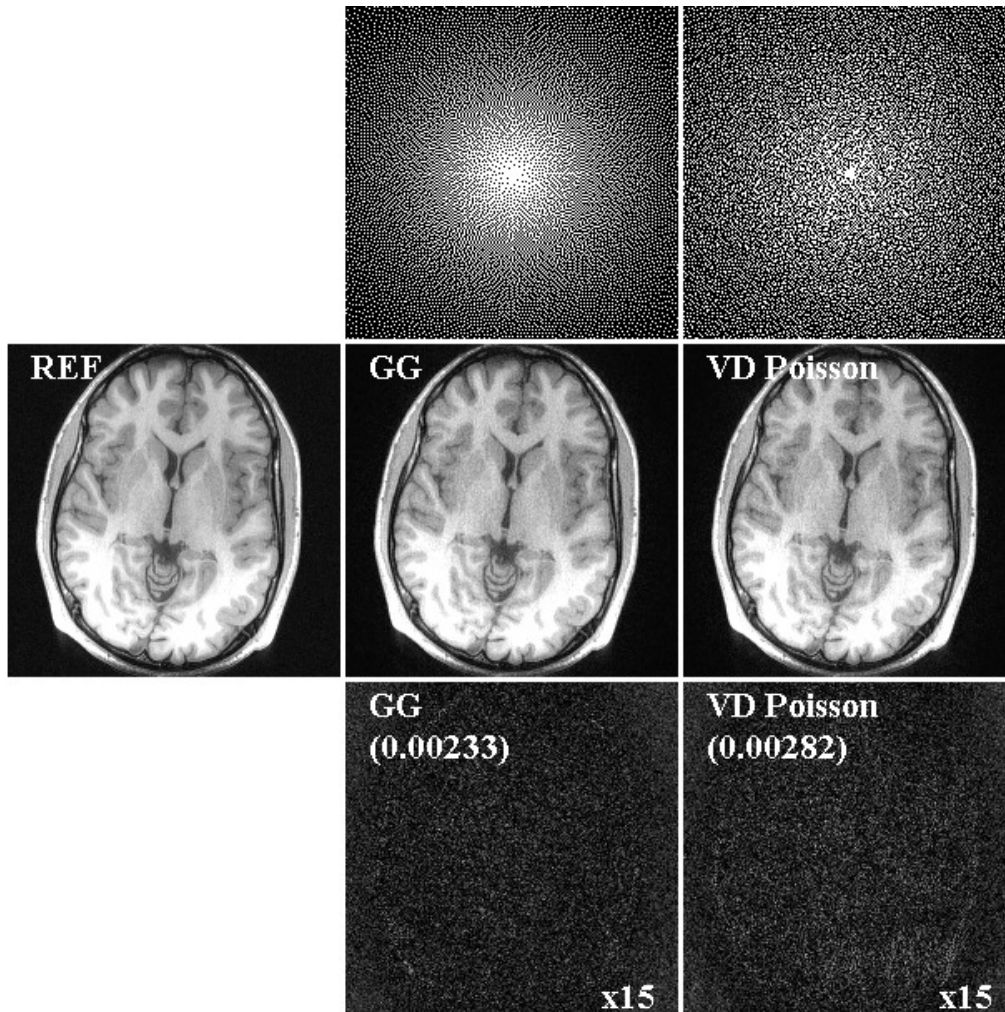


(a)

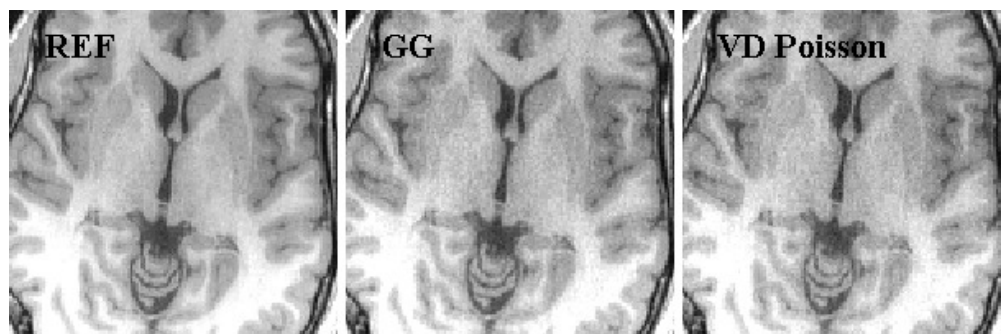


(b)

Figure 7. Comparison of SAKE reconstruction: (a) NMSEs and (b) maximum correlations using VD Poisson disk sampling of Shin, μ -law, and the proposed GG masks as a function of the reduction factor R .

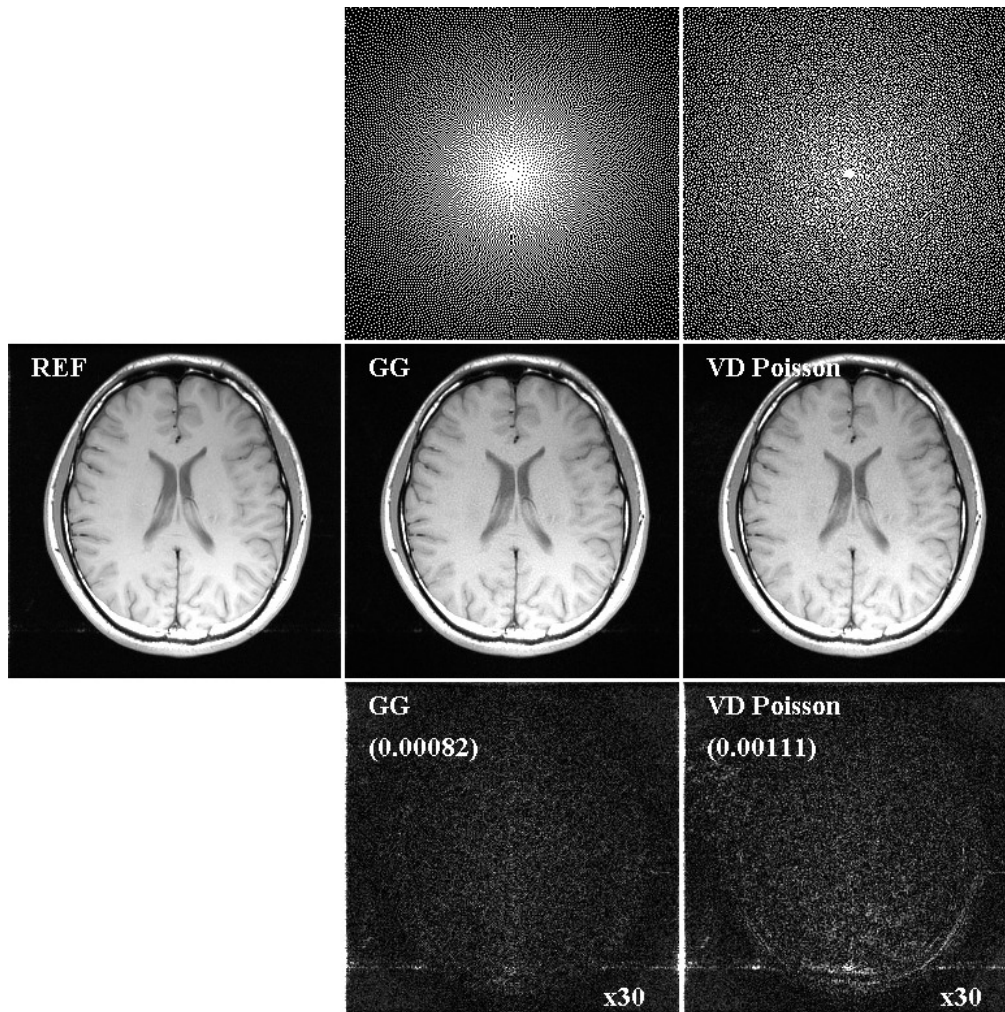


(a)

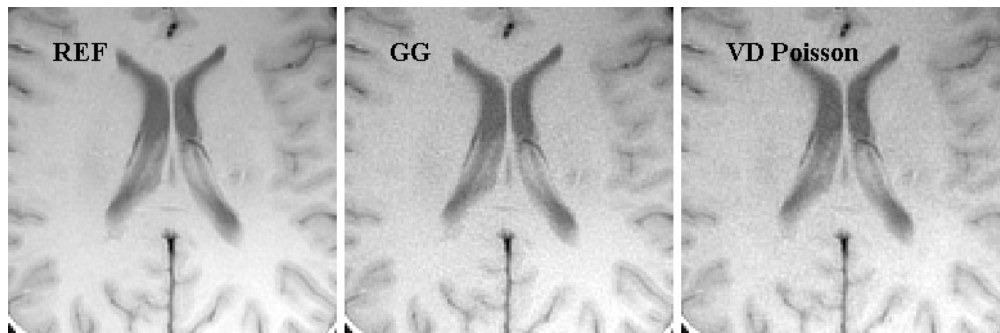


(b)

Figure 8. For the first dataset at $R=3$, (a) sampling mask (top), reference and reconstructions (middle), and the corresponding error images (bottom), (b) reconstructions in region of interest.



(a)



(b)

Figure 9. For the second dataset at $R=3$, (a) sampling mask (top), reference and reconstructions (middle), and the corresponding error images (bottom), (b) reconstructions in region of interest.

5. ACKNOWLEDGEMENT

The authors would like to thank Dr. Shin for providing the VD Poisson disk sampling masks, brain data set, and the SAKE code. The brain data set and the SAKE code are available at <http://www.eecs.berkeley.edu/~mlustig/Software.html>. We would also like to thank Dr. Dunbar for making the Poisson disk generation code available online at <http://www.cs.virginia.edu/~gfx/pubs/antimony/>.

REFERENCES

- [1] Donoho, David L. "Compressed sensing." *Information Theory, IEEE Transactions on* 52.4 (2006): 1289-1306.
- [2] Lustig, Michael, et al. "Compressed sensing MRI." *Signal Processing Magazine, IEEE* 25.2 (2008): 72-82.
- [3] Lustig, Michael, David Donoho, and John M. Pauly. "Sparse MRI: The application of compressed sensing for rapid MR imaging." *Magnetic resonance in medicine* 58.6 (2007): 1182-1195.
- [4] Nayak, KRISHNA S., and Dwight G. Nishimura. "Randomized trajectories for reduced aliasing artifact." *Proceedings of the 6th Annual Meeting of ISMRM, Sydney, Australia*. 1998.
- [5] Lustig, M., et al. "L1 SPIR-iT: Autocalibrating parallel imaging compressed sensing." *Proc Intl Soc Mag Reson Med*. Vol. 17. 2009.
- [6] Vasanawala, S. S., et al. "Practical parallel imaging compressed sensing MRI: Summary of two years of experience in accelerating body MRI of pediatric patients." *Biomedical Imaging: From Nano to Macro, 2011 IEEE International Symposium on*. IEEE, 2011.
- [7] Ying, Xiang, et al. "An intrinsic algorithm for parallel poisson disk sampling on arbitrary surfaces." *Visualization and Computer Graphics, IEEE Transactions on* 19.9 (2013): 1425-1437.
- [8] Knoll, Florian, et al. "Adapted random sampling patterns for accelerated MRI." *Magnetic resonance materials in physics, biology and medicine* 24.1 (2011): 43-50.
- [9] P.J. Shin, P.E.Z. Larson, M. A. Ohliger, M. Elad, J.M. Pauly, D.B. Vigneron, M. Lustig, "Calibrationless parallel imaging reconstruction based on structured low-rank matrix completion," *Magn Reson Med*. online 2013.
- [10] M.N. Do and M. Vetterli, "Wavelet-based texture retrieval using generalized Gaussian density and Kullback-Leibler distance," *IEEE Trans. Image Processing*, pp. 146-158, vol. 11, no. 2, Feb. 2002.
- [11] M.A. Griswold, P.M. Jakob, R.M. Heidemann, M. Nittka, V. Jellus, J. Wang, B. Kiefer, and A. Haasel "Generalized Autocalibrating Partially Parallel Acquisitions (GRAPPA)," *Magn Reson Med*. 2002;47:1202-1210.
- [12] N.S. Jayant and P. Noll, *Digital Coding of Waveforms – Principles and Applications to Speech and Video*, Prentice-Hall, 1984.
- [13] D. Dunbar and G. Humphreys, "A spatial data structure for fast Poisson-disk sample generation," presented at the SIGGRAPH, Boston, MA, Jul.-Aug. 30–3, 2006.
- [14] Chang, Yuchou, Dong Liang, and Leslie Ying. "Nonlinear GRAPPA: A kernel approach to parallel MRI reconstruction." *Magnetic Resonance in Medicine* 68.3 (2012): 730-740.
- [15] Candès, Emmanuel J., and Michael B. Wakin. "An introduction to compressive sampling." *Signal Processing Magazine, IEEE* 25.2 (2008): 21-30.